Canadian Science Publishing
NRC Research Press journals | Publishing Services

Canadian Journal of Physics
Revue canadienne de physique

Spectroscopic Analysis of $CdCl_2$ doped PVA-PVP Blend Films

Journal:	*Canadian Journal of Physics*
Manuscript ID	cjp-2016-0848.R2
Manuscript Type:	Article
Date Submitted by the Author:	02-Mar-2017
Complete List of Authors:	Baraker, Basavarajeshwari; Karnatak University's Karnatak Science College, Dharwad, Physics Lobo, Blaise; Karnatak University's Karnatak Science College, Dharwad, Physics;
Keyword:	PVA-PVP blend, Cadmium Chloride, FTIR, Raman, Fluorescence
Please Select from this Special Issues list if applicable:	N/A

Spectroscopic Analysis of $CdCl_2$ doped PVA-PVP Blend Films

Basavarajeshwari M. Baraker[1] and Blaise Lobo[1*]

[1]Department of Physics, Karnatak University's Karnatak Science College, Dharwad 580 001, Karnataka, India

[*]E- Mail: blaise.lobo@gmail.com

Abstract: The changes in molecular chemical structure of polyvinyl alcohol (PVA) and polyvinyl pyrrolidone (PVP), caused by doping PVA-PVP blend with cadmium chloride ($CdCl_2$), have been studied using UV-Visible (UV-Vis) spectroscopy, Fourier Transform Raman spectroscopy and Fourier Transform Infrared (FTIR) spectroscopy. The formation of cadmium nano-structures and microstructures in $CdCl_2$ doped PVA-PVP blend has been visualized using Scanning Electron Microscopy (SEM), in the range of doping levels varying from 0.5 wt% up to 10.2 wt% (doping level in weight percentage). The incorporation of dopant in PVA-PVP blend is confirmed using Energy Dispersive x-ray Spectroscopy (EDS). The optical absorbance (UV-Vis) spectra of PVA-PVP blend films doped with $CdCl_2$ from 0.5 wt% up to 2.2 wt%, showed a prominent absorption hump with peak at the wavelength 370 nm, in addition to other intermediate energy bands caused by the interactions of $CdCl_2$ with molecules of PVA and PVP. The photo-luminescence (emission/ fluorescence) spectra show significant quenching of fluorescence in $CdCl_2$ doped PVA-PVP blend films. Analysis of FTIR and Raman spectra suggest the possible modes of interaction of cadmium ions (Cd^{2+}) and chlorine ions (Cl^-) with reactive functional groups (C-N, hydroxyl and carbonyl groups) of polymeric molecules in the blend. A reaction scheme for interaction of $CdCl_2$ with PVA-PVP blend is proposed, on the basis of spectroscopic studies on these films.

Key words: PVA-PVP blend, Cadmium Chloride, FTIR, Raman, Fluorescence, UV Visible spectroscopy.

1. Introduction

Experimental studies on the structure and properties of metal salt doped polymeric materials have assumed importance due to their potential applications (as solid polymeric electrolyte (SPE)) in batteries, fuel cells, display devices and gas sensors [1-4]. Incorporation of metal salt in a polymeric system could result in microstructural changes in the host polymer, and consequently, this affects the physical and chemical properties of the polymeric material. Researchers have studied the effect of inorganic salts on the microstructure and properties of hydrophilic polymeric materials [5-8].

Poly vinylalcohol (PVA) is a semi-crystalline polymeric material, whereas polyvinyl pyrrolidone (PVP) is an amorphous polymeric material. PVA and PVP have been studied rigorously by many researchers, because they possess desirable properties like water solubility,

charge storage capacity and good film formation ability. The use of blending and doping techniques for preparing a polymeric material usually results in a new material with enhanced electrical conductivity (due to modified band structure) and changes in other physical properties. These changes depend on the chemical behavior of the dopant, mainly the way in which it interacts with polymeric molecules of the host [9, 10]. The doping of metal salts in a polymer blend is more complicated when compared to that in a homo-polymeric host, because the effect of dopant ions on each component of the blend needs to be considered. The effect of doping polymeric blends with different chemical agents (reduction / oxidation agents) has been a matter of contemporary research interest. In particular, the effects of metal ions on the structure and properties of polymeric blends have been investigated by several researchers [11-13].

Cadmium chloride ($CdCl_2$) is a hygroscopic, crystalline compound (inorganic metallic salt) comprising of cadmium (Cd) and chlorine (Cl). It is highly soluble in water. Cadmium has a significant neutron absorption cross-section, and is useful as a neutron shielding material. Hence, a polymeric material comprising cadmium salt as a dopant assumes significance as a radiation shielding material [14, 15]. It is to be noted that certain compounds of cadmium, when added to plastics (PVC), results in stabilizing (light, heat and weathering stabilization) of the compounded polymeric material [16]. Also, filling $CdCl_2$ in polyvinyl chloride (PVC) has been shown to result in degradation of the polymeric material [17, 18].

Significant changes are observed in the microstructure and properties of PVA-PVP blends doped with $CdCl_2$, the details of which have been published elsewhere [19-21]. At low concentrations of $CdCl_2$, from 0.5 wt% up to 2.2 wt%, cadmium nano-structures in the form of nano-spheres and nano-rods are observed in SEM micrographs of the $CdCl_2$ doped PVA-PVP blend films. At 3.3 wt% doping level, a network of complex structural features is observed. It is interesting to note that, these nano-structural features hinder the motion of mobile charge carriers in the polymeric material, and this is manifested as an increase in electrical resistivity of the sample (observed for doping levels ranging from 0.5 wt% up to 3.3 wt%) [19]. At doping levels varying from 4.4 wt% up to 7.2 wt%, flower shaped nanostructures are seen in the SEM images. However, at 10.2 wt% doping level, micro-globules of the dopant are seen in the polymeric host, which disintegrate at dopant concentration of 12.1 wt%, yielding a homogeneous morphology at 15.5 wt% and above [20]. These changes in micro-structural features (visualized using SEM images) are accompanied by significant changes in degree of crystallinity of the doped blend, as evidenced by XRD and DSC scans of the sample (details are presented/ published elsewhere) [19, 21]. The microstructural analysis of $CdCl_2$ doped PVA-PVP blend films suggests that it can be used as SPE for films with $CdCl_2$ doping level above 15.5 wt%, when the sample is completely amorphous. Nanda Prakash et al [22] have suggested that $CdCl_2$ doped PVA is a SPE which is suitable for energy storage devices (like batteries / fuel cells). The study of AC conductivity properties of $CdCl_2$ filled PVA-PVP blend by Pandey et al [23, 24] has revealed that this composite is suitable for application as a SPE, due to its desirable electrical impedance and conductivity properties.

The spectroscopic investigation of $CdCl_2$ doped PVA-PVP blend films will contribute to an understanding of this doped polymeric system; especially, with regard to chemical structural changes taking place in molecules of the polymeric blend (PVA and PVP), due to doping (with $CdCl_2$). Using FTIR spectra and Fourier Transform (FT)-Raman spectra, the fundamental modes of vibration are observed at different frequencies, due to induced dipole moment and polarization effect in the material, respectively [25]. In addition, absorbance and photoluminescence spectra have also been studied, in order to analyze the structural modifications and formation of charge transfer complexes in the doped polymeric material.

2. Materials and Methods

2.1.Materials

Semicrystalline PVA (1,40,000 molecular weight), amorphous PVP (50,000 molecular weight) and cadmium chloride monohydrate ($CdCl_2.H_2O$) were purchased from HiMedia Laboratories Pvt. Ltd, Mumbai.

2.2.Sample Preparation

Solution casting method was used in order to prepare $CdCl_2$ doped PVA-PVP blend films. In the first step, aqueous solutions of PVA-PVP blend were prepared in different beakers. In order to do this, two grams each of PVA and PVP were taken in each beaker, and the mixture was dissolved in 100 ml of double distilled water. Translucent, homogeneous solutions of PVA-PVP blend were obtained, by stirring the mixtures (taken in different beakers) continuously for more than 24 hours, using magnetic stirrers. The standard solution of $CdCl_2$ was obtained by dissolving $CdCl_2.H_2O$ in double distilled water. Different volumes of this standard solution were added to PVA-PVP aqueous solutions kept ready in different beakers, in order to prepare the $CdCl_2$ doped PVA-PVP aqueous blend solutions, with doping levels varying from 0.5 wt% up to 21.5 wt%. After doping, contents of the different beakers were stirred in order to get homogeneous aqueous solutions of the $CdCl_2$ doped PVA-PVP blend. After stirring and filtering, contents of the beakers were poured into properly labelled glass petridishes, which were then kept inside an air cooled oven maintained at 40℃ (for evaporation of the solvent). After fifteen days, dry films were peeled off carefully from the glass substrates and then stored in a desiccator, in order to avoid absorption of ambient moisture. The $CdCl_2$ doping level (*DL*) in each film was calculated using equation (1).

$$DL(wt\%) = \frac{M_d}{M_d+M_p} \times 100 \qquad (1)$$

In equation (1), M_d is the weight of dopant ($CdCl_2$) and M_p is the weight of the polymer blend (PVA+PVP).

2.3. Characterization Methods

NXR FT-Raman module spectrometer, at 4 cm^{-1} resolution, was used to acquire Raman spectra of the $CdCl_2$ doped PVA-PVP blends films in the wavenumber range 100-3750 cm^{-1}.

FTIR spectra of $CdCl_2$ doped PVA-PVP blends were recorded in the wavenumber range 400-4000 cm^{-1}, using NICOLET 6700 FTIR Spectrometer, by following the potassium bromide (KBr) pellet method.

3. Results and Discussion

3.1 FT- Raman Spectroscopy

The different modes of molecular vibration, namely, stretching, bending, scissor, twisting and wagging motions of different molecular groups in $CdCl_2$ doped PVA-PVP blend have been studied. Raman spectroscopy has been used to study the interaction of cadmium containing chemical species with PVA [26] and PVP [27]. Raman spectra, at different concentrations (expressed in weight percentage (wt%)) of $CdCl_2$ in PVA-PVP blend films, are shown in fig. 1. The inter-molecular and intra- molecular interactions in PVA, PVP and $CdCl_2$ have been investigated (see fig. 2: interaction/ reaction scheme).

CH_2 symmetric stretch:

In the Raman spectra, a sharp peak is observed at 2920 cm^{-1} (see fig.1a), which is attributed to CH_2 symmetric stretch in the polymer chains. At 0.0 wt% of $CdCl_2$ in PVA-PVP (that is, pure or un-doped) blend, this peak is at 2921 cm^{-1}. There is significant variation in peak intensity, rather than wavenumber, in all doped samples. The decrease in full width at half maximum (FWHM) of this peak, from doping level 0.5 wt% up to 6.3 wt% is a result of electrical interactions between hydroxyl (OH) group and carbonyl group (C=O) with Cd^{2+} and Cl^- ions.

C=O stretching

The most prominent vibration in $CdCl_2$ doped PVA-PVP blend films is carbonyl (C=O) stretching due to both the acetyl group of un-hydrolyzed PVA and carbonyl group in the lactum ring of PVP. The vibration at 1660 cm^{-1} is attributed to carbonyl group in PVP, which is observed as a weak peak in fig.1b. This reveals that PVP is involved in the formation of charge transfer complexes by transferring electron/ electrons from lactum ring [28] to Cd^{2+} / Cl^- ions of $CdCl_2$, (see reaction scheme; Fig. 2). Hence, there is an increase in degree of crystallinity of the doped blend films, from 0.5% up to 6.3%, in the lower dopant concentration region (confirmed using XRD; details published elsewhere [19]); this is also reflected in the FTIR spectra. The decrease in FWHM of this peak at lower dopant levels reveals that, since sufficient ions of dopant (both cations (Cd^{2+}) and anions (Cl^-)) are available in the films to interact with the electronegative oxygen (O^-) and electropositive nitrogen (N^+) atom of PVP and to form nano-clusters of the dopant in the PVA-PVP matrix. These nanostructures are visualized in the SEM images of the $CdCl_2$ doped PVA-PVP blend films (see reference [19] and fig. 4 a-e (SEM images

inset)). At higher concentration (above 10.2%) of $CdCl_2$ in PVA-PVP blend, there is a significant decrease in intensity and a shift in wavenumber (refer table.1) due to carbonyl group, which is because of reduced molecular interactions between $CdCl_2$ and PVA-PVP matrix. The peak at 1730 cm^{-1} is attributed to carbonyl (C=O) stretching, due to the acetyl group of un-hydrolyzed PVA.

C-O stretch and CH_2 scissor:

In fig.1 (a-b), the peak around 1430 cm^{-1} is attributed to both C-O stretch and CH_2 scissor. The peaks at 1437 cm^{-1} and 1436-1444 cm^{-1} are seen in both pure and doped PVA-PVP blends, respectively. The intensity of this peak, and the variation of full width at half maximum (FWHM) of its profile is suggestive of a change in functional group from C=O to C-O in PVP and acetyl groups of unhydrolyzed PVA by transferring an electron, while interacting with the dopant ions (see resonance structure in the reaction scheme; Fig. 2).

CH-OH bending and C-H bending:

The just resolved peak at 1360 cm^{-1} corresponds to C-H bending in pure PVA-PVP blend, and varies between 1360-1375 cm^{-1} in $CdCl_2$ doped PVA-PVP samples due to inter/intra molecular interactions. A shoulder to C-H bending peak is seen at 1300 cm^{-1} (see fig.1b), which is due to CH-OH bending in PVA during intra-molecular interactions in PVA and intermolecular interactions in PVA-PVP blend (see reaction scheme; fig. 2). CH-OH bending is a result of electrical interactions between Cd^{2+}/Cl^- ions and PVA-PVP polymer matrix [29]. This peak is observed at 1301 cm^{-1} in pure PVA-PVP blend, and varies from 1308 cm^{-1} up to 1317 cm^{-1} in the doped samples. The CH-OH bending in $CdCl_2$ doped PVA-PVP is due to formation of charge transfer complexes (such as, PVA+Cd^{2+}/Cl^-) by intermolecular interactions between PVA-PVP blend and the dopant (Cd^{2+} and Cl^-) ions.

C-C chain, ring and breathing:

The three different peaks at 750 cm^{-1}, 848 cm^{-1} and 920 cm^{-1} (see fig.1c) are due to C-C chain in polymer backbone. In doped polymers, the peak frequencies (actually, wavenumbers) vary between 747-762 cm^{-1}, 848-854 cm^{-1} and 923-939 cm^{-1}. The variation of peak intensity in doped samples confirms chemical structure modification due to inter/intra molecular interactions between $CdCl_2$ and PVA/ PVP molecules of the polymeric blend.

LO phonon vibrons (vibrations):

In Raman spectra, a strong peak is observed at frequency 163 cm^{-1} in $CdCl_2$, and at 179 cm^{-1} in pure (un-doped) PVA-PVP blend films. This peak varies in wavenumber, from 179 cm^{-1} up to 183 cm^{-1} in $CdCl_2$ doped PVA-PVP blend films. No significant shift in wavenumber is observed, but increased FWHM of this peak (see fig.1c) is seen from 0.5 wt% up to 6.3 wt%, which decreases in the samples doped from 10.2 wt% up to 21.5 wt%. This peak is attributed to first overtone harmonic of longitudinal optical (LO) phonon effect [30]; υ_{LO} and υ_{2LO} are at 322 cm^{-1} and 355 cm^{-1} in pure $CdCl_2$ and pure PVA-PVP blend, respectively. In the case of pure $CdCl_2$,

the peak at 220 cm^{-1} is assigned to Cd-Cl stretching. The peaks due to cadmium and chlorine ions in PVA-PVP matrix have been assigned [31, 32].

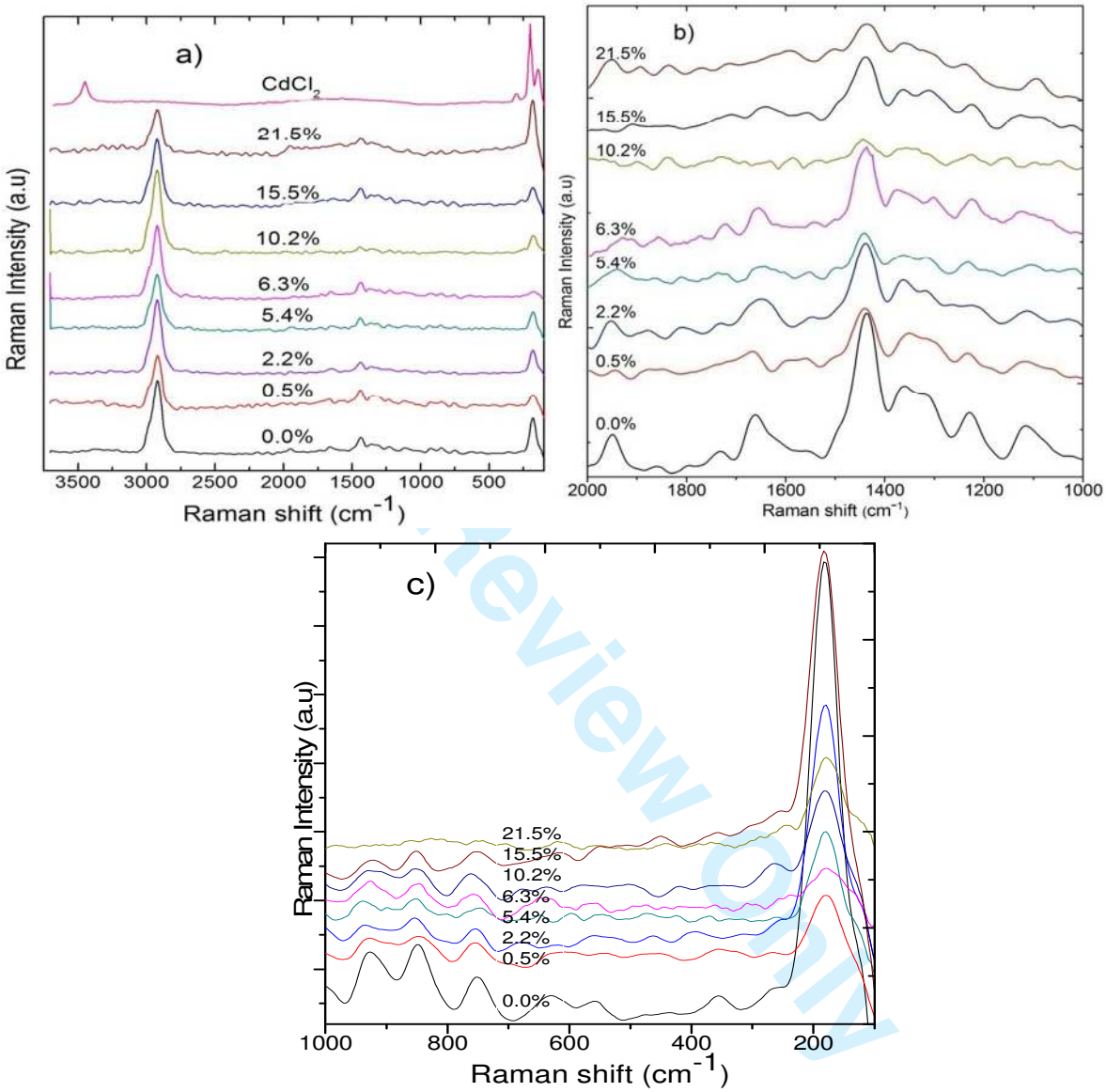

Figure 1: Raman spectra at different concentrations (expressed in weight percentage (wt%)) of $CdCl_2$ in PVA-PVP blend films. (a) Raman spectra of the $CdCl_2$ doped PVA-PVP blend films in the entire wavenumber range, from 100 cm^{-1} up to 3750 cm^{-1}. (b) Raman spectra of the $CdCl_2$ doped PVA-PVP blend films in the wavenumber range of interest, from 1000 cm^{-1} up to 2000 cm^{-1}. (c) Raman spectra of the $CdCl_2$ doped PVA-PVP blend films in the wavenumber range of specific interest, from 100 cm^{-1} up to 1000 cm^{-1}.

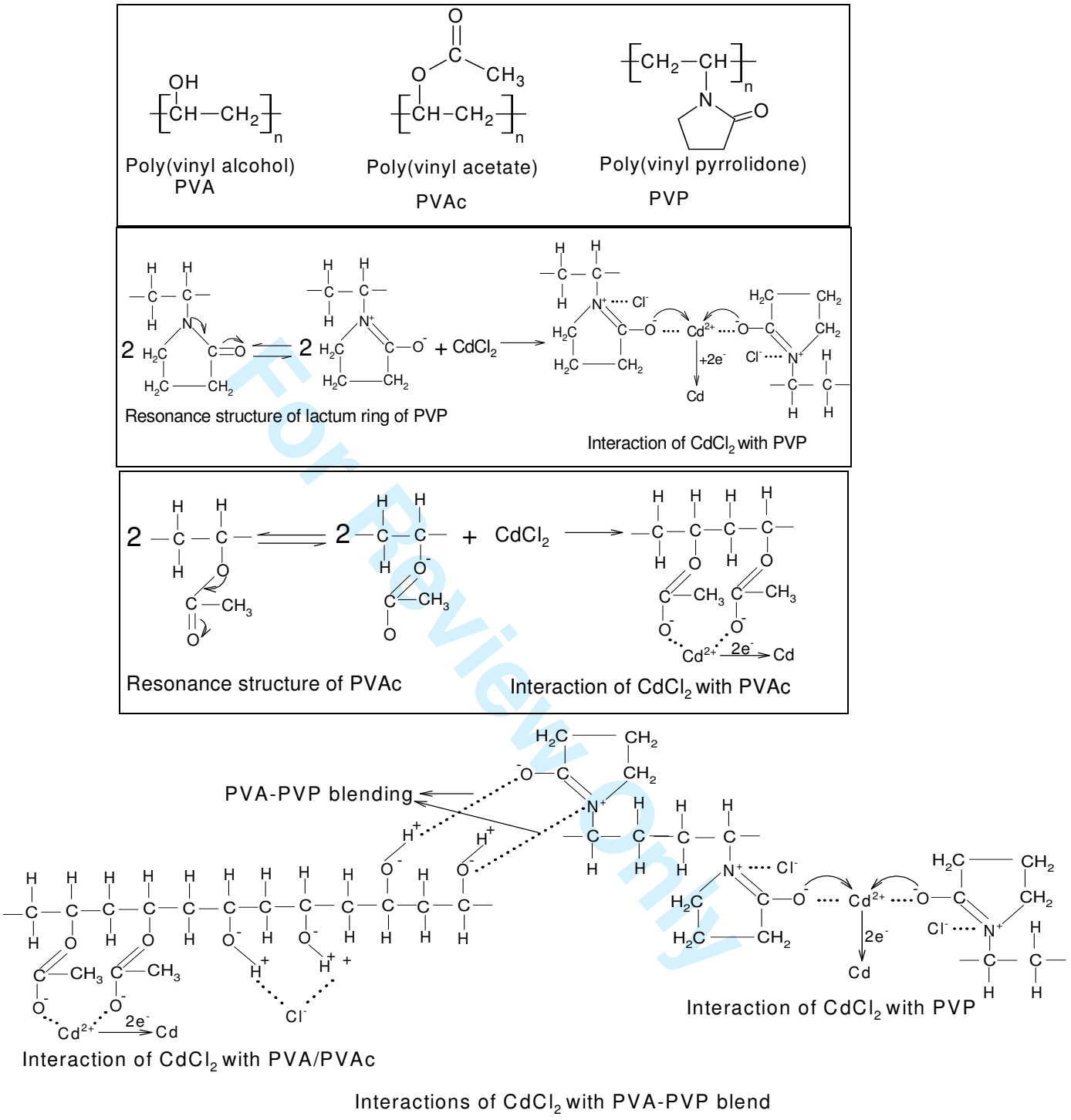

Figure 2: Reaction schemes, suggesting possible modes of chemical interaction between dopant ions (Cd^{2+} and Cl^{-}) and polymer molecules (PVA and PVP molecules), in addition to inter/ intra- molecular hydrogen bond interactions in the PVA-PVP blend films.

The discussion on Raman spectra reveals that $CdCl_2$ doped PVA-PVP blends are hybrid materials with modified properties caused by the formation of charge transfer complexes and nano-structures (see SEM images inset in fig.4., a-e). These nano-clusters increases the degree of crystallinity of $CdCl_2$ doped PVA-PVP films, in the range of dopant levels varying from 0.5 wt% up to 6.3 wt%. At the higher dopant levels (10.2 wt% and above) of $CdCl_2$, enhancement in amorphousness and reduced molecular interactions have been observed. The wavenumber of each absorbance peak corresponds to a particular mode of vibration. These peak assignments are listed in table 1. These peaks are attributed to different molecular vibrations, which are in agreement with similar assignments made by other researchers [33-36].

3.2 FT-IR Spectroscopy

As a supportive study for Raman spectroscopy, FTIR spectra have been analyzed in order to confirm changes in the chemical structure of polymer molecules in $CdCl_2$ doped PVA-PVP blend, due to ion and atomic/ molecular interactions.

O-H stretch

In fig. 3, the strong and broad absorption band at 3440 cm^{-1} in the FTIR scan of (un-doped) PVA-PVP is assigned to O-H stretching vibration (of hydroxyl groups of PVA) and the OH stretching vibration of the absorbed water, since PVP is highly hygroscopic. The broad nature of this band is a measure of the hydrogen bond interactions (inter/intra molecular) involving the hydroxyl groups of PVA. The decrease in intensity and displacement in wave number of this peak, from 3424 cm^{-1} up to 3448 cm^{-1} in $CdCl_2$ doped PVA-PVP blends reveals the formation of charge transfer complexes due to inter/intra molecular interaction between PVA and dopant ions Cd^{2+} / Cl^- , involving the hydroxyl group of PVA (see reaction scheme in fig.2).

CH_2 asymmetric and symmetric stretch

The band corresponding to CH_2 asymmetric stretching vibration occurs at 2960 cm^{-1} and CH_2 symmetric stretching vibration at 2924 cm^{-1}. The shift in their values after doping (see table 1) is attributed to structural modifications of PVA-PVP backbone, while interacting with $CdCl_2$.

Carbonyl (C=O) stretch

The band at 1733 cm^{-1} corresponds to carbonyl stretching of acetyl group of unhydrolyzed PVA (i.e., partially hydrolyzed portions of PVA molecules) [37], and that at 1665 cm^{-1} corresponds to carbonyl (C=O) group of PVP [38]. The dominant peak at 1665 cm^{-1} (in fig.3) confirms that PVP is more interactive (with $CdCl_2$) when compared with PVA. Since PVP has the ability to form a capping over the ions/atoms of Cd^{2+}/Cd, it is proposed there is electron transfer from O^- ions to Cd^{2+} ion to form Cd atom, as shown in reaction scheme (see fig. 2). Since PVA is partially hydrolyzed, a weak peak appears at 1730 cm^{-1} due to molecular interactions of the chromophores (C=O) present in the acetyl group of PVA (which is not fully hydrolyzed) with the dopant ions.

The variation in intensity and wavenumber of this vibration indicates formation of charge transfer complexes (such as PVP+Cd^{2+} and PVA+Cd^{2+}); the transfer of electrons from polymeric molecules (PVA and PVP) to Cd^{2+} leads to formation of Cd atoms, which evolve (aggregate) to form cadmium nano-structures in the $CdCl_2$ doped PVA-PVP blend films, which are observed using SEM; see Fig. 4 (inset).

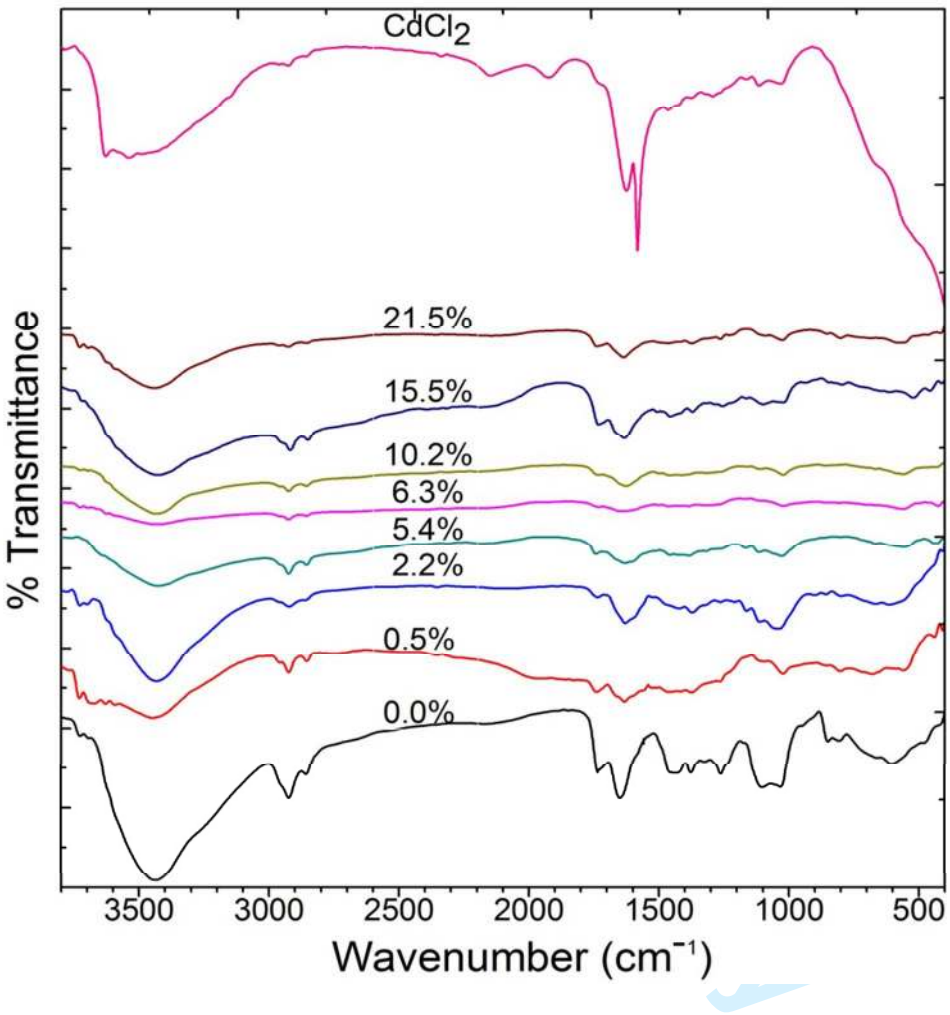

Figure 3: FTIR spectra at different concentrations (expressed in weight percentage (wt%)) of $CdCl_2$ in films of PVA-PVP blend.

C-N stretch and CH_2 wagging

The peak at 1260 cm^{-1} is due to C-N stretch in lactum ring of PVP and also CH_2 wagging in PVA-PVP backbone. Since PVP contains C-N linkage, there could be interactions of N^+ with Cl^- ion of dopant as shown in the reaction scheme (see fig. 2), Hence, there is considerable shift in both the wave-number corresponding to C-N absorbance, in both FTIR and Raman spectra of $CdCl_2$ doped PVA-PVP blend films. The sharp band at 1030 cm^{-1} in pure PVA-PVP blend corresponds to C-N vibrations in PVP, and shift of this peak between 1020 cm^{-1} to 1044 cm^{-1} indicates the formation of charge transfer complexes, as illustrated in resonance structure of PVP

(in reaction scheme; see fig. 2) and due to inter-molecular and molecule –ion interactions; for example, PVP + Cl^-.

N-C=O bend, ring deformation

The broad peaks at 550 cm^{-1} and 650 cm^{-1} in pure PVA-PVP blends have been assigned to N-C-O bend and ring deformation, the peak frequencies (actually, wavenumbers) vary from 515 - 550 cm^{-1} and 613 - 650 cm^{-1} at different concentrations of dopant ($CdCl_2$) in the PVA-PVP blends (due to inter/ intra-molecular interactions). The shift in vibration frequency associated with stretching, wagging, twist and other phenomenon in $CdCl_2$ doped samples are due to intra/inter molecular hydrogen bonding with the adjacent OH group of PVA. All possible structural deformations are assigned at different frequencies, and the same is listed in table1 (and seen in fig. 3). Due to these molecular interactions, there are chemical/ structural changes which lead to microstructural modifications in $CdCl_2$ doped PVA-PVP blend films. These changes also affect the band structure of $CdCl_2$ doped PVA-PVP blend films.

3.3.Energy Dispersive X-ray Spectroscopy (EDS)

Energy Dispersive X-ray Spectrometry (EDS) is an analytical technique for determination of the elemental constituents in a sample (material). In the recorded EDS spectra of $CdCl_2$ doped PVA-PVP blends (shown in fig. 4), it is observed that there are five cadmium (Cd) peaks and two chlorine (Cl) peaks, which confirm the presence of dopant atoms in films of the doped polymeric blend. Since Carbon (C), Nitrogen (N) and Oxygen (O) atoms are present in the parent (original polymer) chains of PVA/PVP blend, the peaks corresponding to these elements are also observed in the EDS spectra of $CdCl_2$ doped PVA-PVP blend films (see fig.4). With an increase in $CdCl_2$ concentration in PVA-PVP blend, there is an increased intensity of Cd and Cl peaks in the recorded EDS spectra; this reveals the presence of a larger number of dopant ions/atoms in the polymer matrix (doped blend films), at higher doping levels. The peaks due to fluorescence x-rays of Cd, namely, L_I, $L_{\alpha 1}$, $L_{\beta 1}$, $L_{\beta 2,\ 15}$ and $L_{\gamma 1}$ are observed at 2.76 keV, 3.14 keV, 3.35 keV, 3.53 keV and 3.72 keV, respectively. The two x-rays peaks attributed due to Cl are at 2.66 keV and 2.81 keV; they are attributed to $K_{\alpha 1}$ and $K_{\beta 1}$ fluorescence x-rays of Cl.

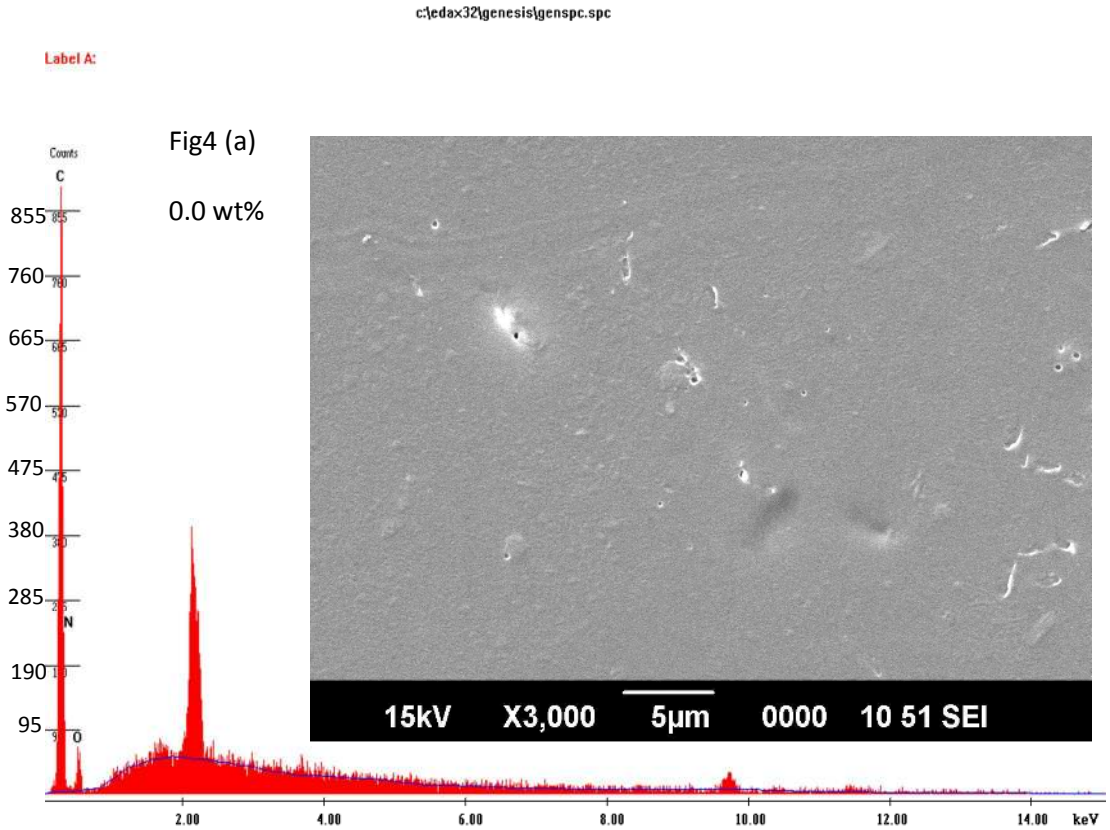

Fig4 (a)

0.0 wt%

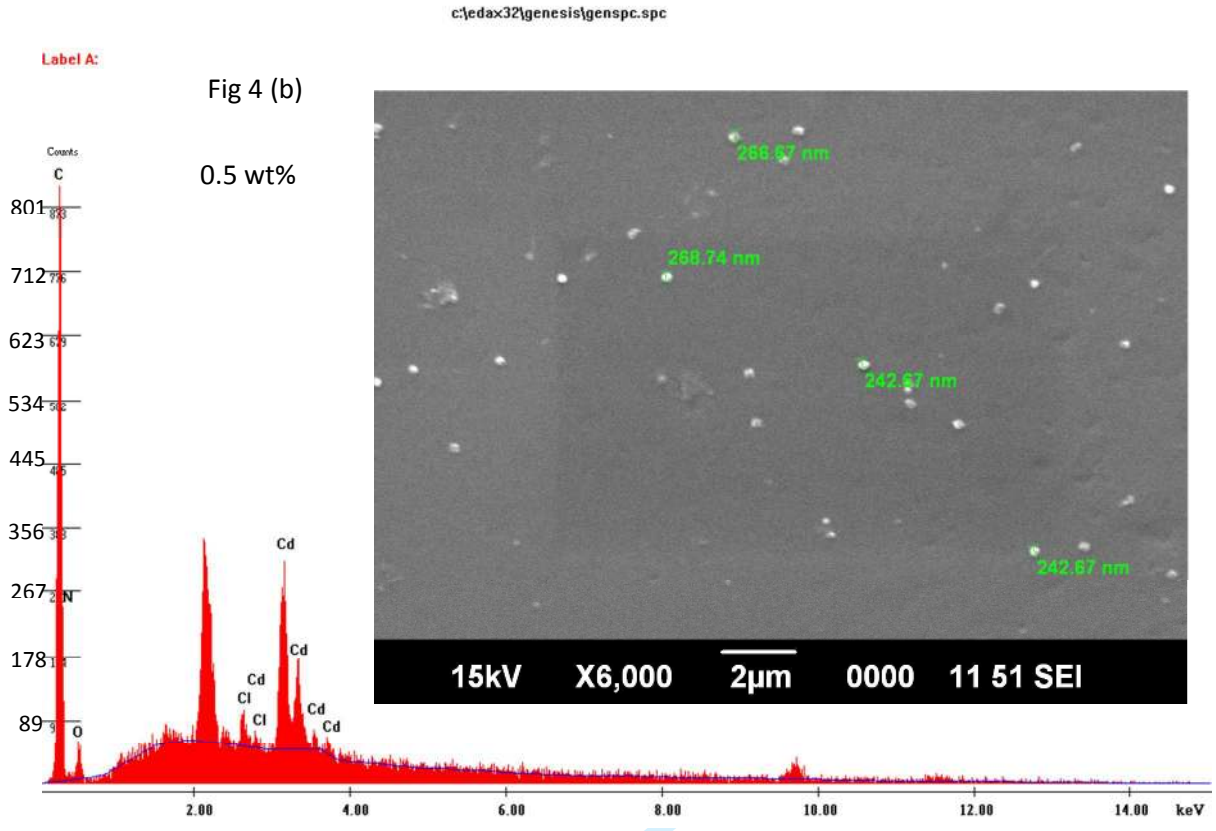

Fig 4 (b)

0.5 wt%

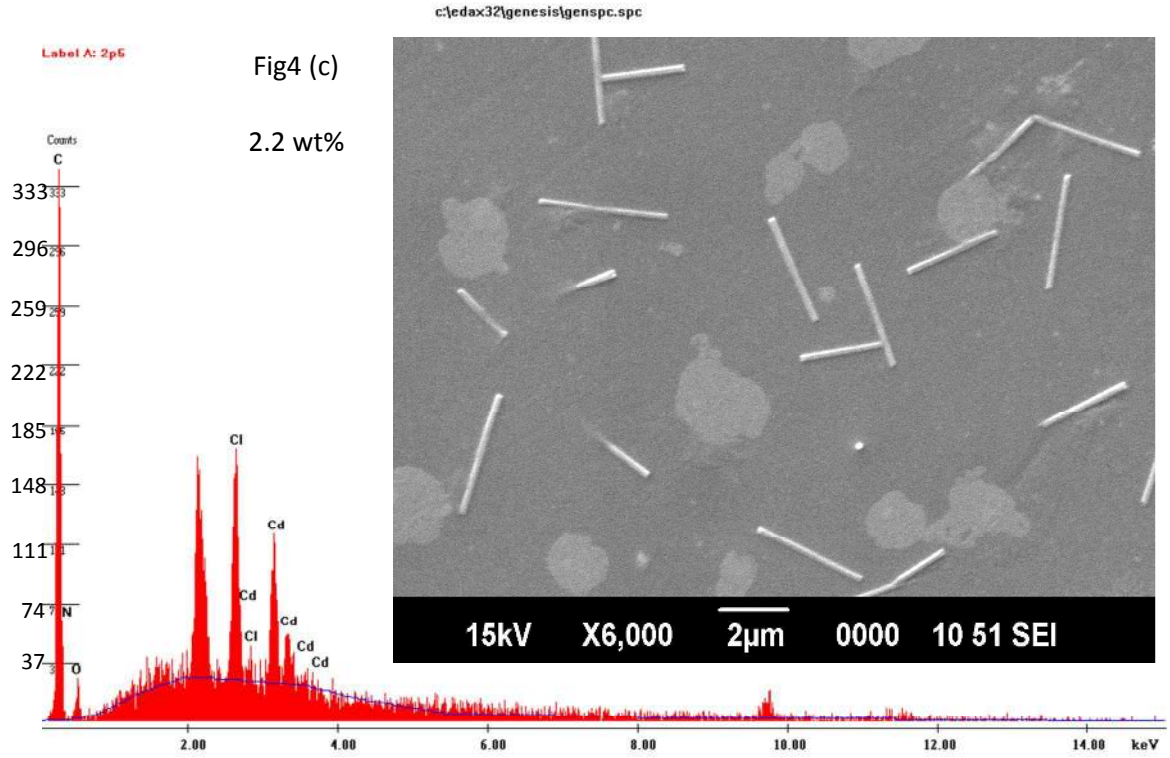

Fig4 (c)

2.2 wt%

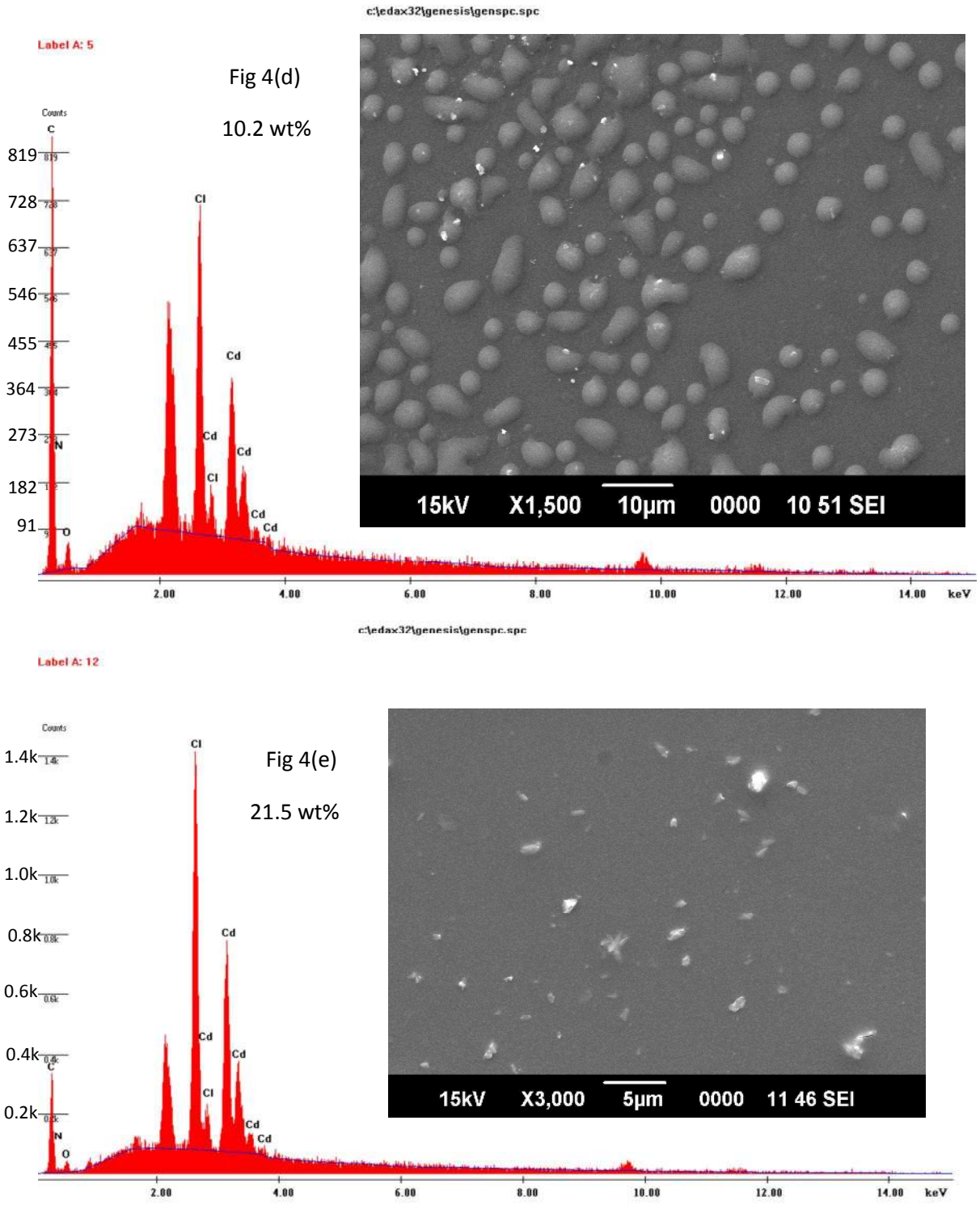

Figure 4: EDS spectra at different concentrations; Fig. 4(a): 0.0 wt% (Pure PVA-PVP blend), Fig. 4(b): 0.5 wt%, Fig. 4(c): 2.2 wt%, Fig 4. (d):10.2 wt% and Fig 4. (e): 21.5 wt% doping level of $CdCl_2$ in PVA-PVP blend films. SEM images for the corresponding doping levels are inset.

3.1 UV-Visible Spectroscopy

The optical absorbance (UV-Vis) spectra of PVA-PVP blend samples doped with $CdCl_2$ from 0.5 wt% up to 2.2 wt% show a prominent absorption hump, with peak at the wavelength 370 nm, in addition to intermediate energy bands, which are caused by the interactions of $CdCl_2$ with molecules of PVA and PVP (See fig. 5). Also, at these doping levels, the SEM images (see inset images in fig. 4 (b, c)) show nanostructures due to dopant; the possibility of localized Surface Plasmon Resonance (LSPR) due to Cd nanostructures causing this absorption hump needs to be discussed. LSPR is the collective oscillations of electrons in metallic nanostructures in the presence of suitable optical excitation energy [39, 40]. The absorption band intensity and wavelength are characteristic of LSPR and which are sensitive to size, size distribution, shape of nanostructures and surrounding medium [41, 42]. The enhanced interest towards study of LSPR by researchers is due to its exploitation in the field of sensors; chemical sensors, biosensors and optical devices [43-46]. The use of a UV-Visible (UV-Vis) spectrometer offers a simple technique for recognition of metallic nano-particles, since they exhibit the phenomenon of LSPR phenomenon, characterized by a strong absorption of electromagnetic (EM) radiation in a certain wavelength range (resonance absorption) of the visible spectrum. On observing intense absorption band at 370 nm, the LSPR is proposed to be due to cadmium nanostructures in $CdCl_2$ doped with PVA-PVP blend. Since LSPR is observed for low doping levels of $CdCl_2$ in PVA-PVP blends, these samples can be used to fabricate sensors. The ongoing research on noble metal nano-particles has gained increased attention of researchers due to enhancement in electric field on their surface and the manner in which these nanostructures affect the local environment. An enhancement in fluorescence intensity is seen for small nanoclusters when compared to bulk. In the case of $CdCl_2$ doped PVA-PVP films, this enhancement in fluorescence intensity is observed in case of films doped to 0.5 wt% doping level (See Fig. 6a). However, fluorescence quenching is observed in case of $CdCl_2$ doped PVA-PVP blend films with doping level above 0.5 wt%. Since self grown nano-rods of larger aspect ratio (length/width) are seen in $CdCl_2$ doped PVA-PVP blend films, fluorescence quenching has been observed, which is attributed to non-radiative energy transfer from excited fluorophore to the cadmium nano-rods. Although PVP plays a major dual role as a reducing and capping agent of cadmium nano-particles, the incorporation of PVA helps in the formation of a self- supporting film (of PVA-PVP blend), on solution casting. The cadmium ions (Cd^{2+}) get converted to cadmium atoms (Cd) by accepting electrons from PVP (as explained in reaction scheme in fig. 2). The size and aspect ratio of nano-spheres is ten times less than that of nano rods (see fig. 5d), which result in decrease in area and full width half maximum (FWHM); these values were estimated by fitting the spectra using multiple Gaussian and Lorentzian shapes to the LSPR absorption band (see table 2, Fig. 5b and Fig. 5c) in the UV-Visible spectra of $CdCl_2$ doped PVA-PVP blend films.

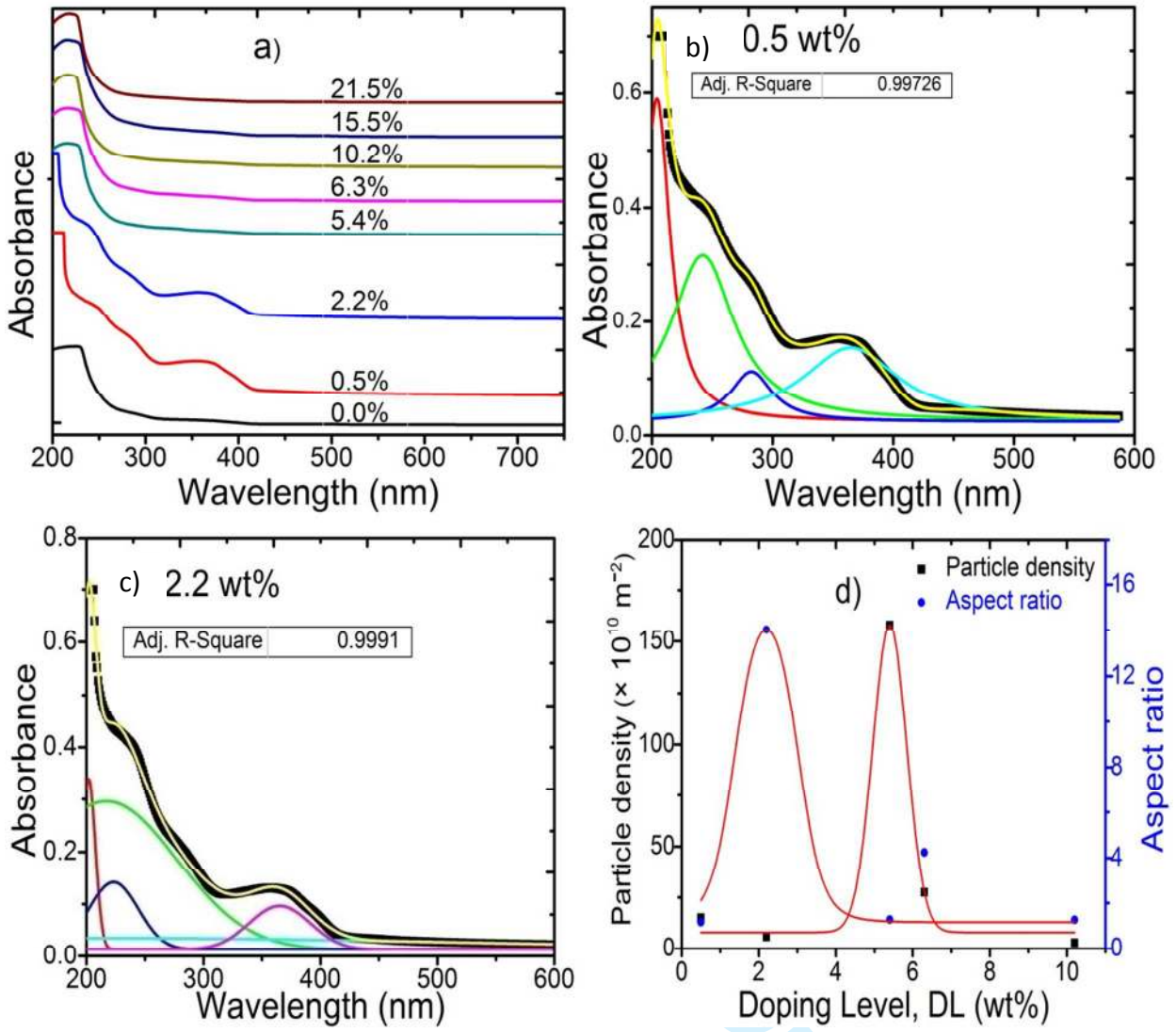

Figure 5: a) Absorbance spectra, at different concentrations of $CdCl_2$ in PVA-PVP blend b) multiple peak Lorentz fitting at 0.5 wt% c) at 2.2 wt% Gaussian model and d) Particle density, Aspect Ratio (from SEM images; See figure 4 (inset images)) with respect to doping level. (In Fig. 5b and Fig. 5c, the actual value of absorbance has been divided by ten).

The high energy absorption edge in UV-Visible spectra of the un-doped and $CdCl_2$ doped PVA-PVP blend films correspond to excitation of electrons from lower energy state (highest occupied molecular orbital, HOMO) to higher energy state (lowest unoccupied molecular orbital, LUMO) by absorbing incident photons of suitable energy. In all the $CdCl_2$ doped PVA-PVP blend films, optical absorption has occurred at 212 nm due to $n \rightarrow \pi^*$ transition, and absorption edge at 220 nm - 270 nm (see fig.5a) is due to $\pi \rightarrow \pi^*$ transition of unsaturated (C=O and C=C) bonds. The presence of multiple intermediate energy bands in the forbidden gap is due to the interaction between dopant ($CdCl_2$) and PVA-PVP, manifested in UV/VIS spectrum by the existence of absorption humps, before the high energy absorption edge.

SEM images were utilized to extract the data required to plot fig. 5d. Some of the SEM images are shown in Fig. 4 (inset). The details of microstructural changes caused in PVA-PVP blend (on doping with $CdCl_2$) have been presented elsewhere [20]. The ratio of length to the breadth is used to calculate aspect ratio of cadmium nanostructures in $CdCl_2$ doped PVA-PVP films, at different doping levels. The variation of the aspect ratio with respect to doping level is shown in fig. 5d. The maximum aspect ratio is observed for 2.2 wt% sample, because of significantly larger length of nanorods, when compared to their diameter. Particle density is determined by counting the number of particles per unit area from SEM images of the doped polymeric blend, for samples doped to different levels. The following procedure was adopted. A circle of radius 'r' was drawn on a photocopy of the recorded SEM image. Then, the number of nano structures (N) inside that circle was counted, and this number was divided by area of the drawn circle. Thus, the analysis required to extract information from SEM images was done manually. Some of the SEM images of $CdCl_2$ doped PVA-PVP films are shown in Fig. 4 (a-e) (inset). It was expected to observe a shift in peak wavelength with increase in size of nano cluster and two absorption bands for nano-rods, corresponding to longitudinal (low-energy) and transverse (high-energy) surface plasmon bands [47, 48]; however, these effects are not observed in case of $CdCl_2$ doped PVA-PVP blend films. Also, the effect of LSPR is not clearly seen for the $CdCl_2$ doped PVA-PVP blend films in the doping range from 5.4 wt% up to 10.2 wt%.

3.4. **Analysis of Photo-luminescence Spectra**

The emission (photo-luminescence) peaks of $CdCl_2$ doped PVA-PVP blend are obtained at the excitation wavelength 355 nm. As seen from fig. 6a, there are two emission peaks at the wavelengths 412 nm and 434 nm, in addition to the just resolved peaks at 458 nm and 463 nm. These fluorescence peaks have been identified by multi-peak Gaussian fitting (see fig.6c illustrated for 5.4 wt%) and listed in table 2. The fluorescence peak at 412 nm is due to fluorophore of complex Cd^{2+}/Cl^{-}+PVP [49] and Cd^{2+}/Cl^{-}+PVA; peaks at 434 nm, 458 nm and 463 nm are due to Cd^{2+}/Cl^{-}+PVA [50]. Since C=O group is present in both PVP and acetyl groups of unhydrolyzed parts of PVA, electron transfer to cadmium ion takes place from both of these molecules. At 0.5 wt% of $CdCl_2$ in PVA-PVP, the fluorescence peak at 434 nm is dominant when compared to the peak at 412 nm, which indicates that the charge transfer complexes formed due to PVA are more available for the excitation.

It is observed that there is enhancement in fluorescence intensity due to smaller size of nano particle at 0.5 wt%. But in the dopant range varying from 2.2 wt% up to 10.2 wt%, the role of PVP is more important. This is confirmed from FTIR spectra; PVP acts as a capping agent by accumulating electrons on the surface of cadmium atoms as evidenced by the enhancement in the peak intensity at 412 nm when compared to that at 434 nm.

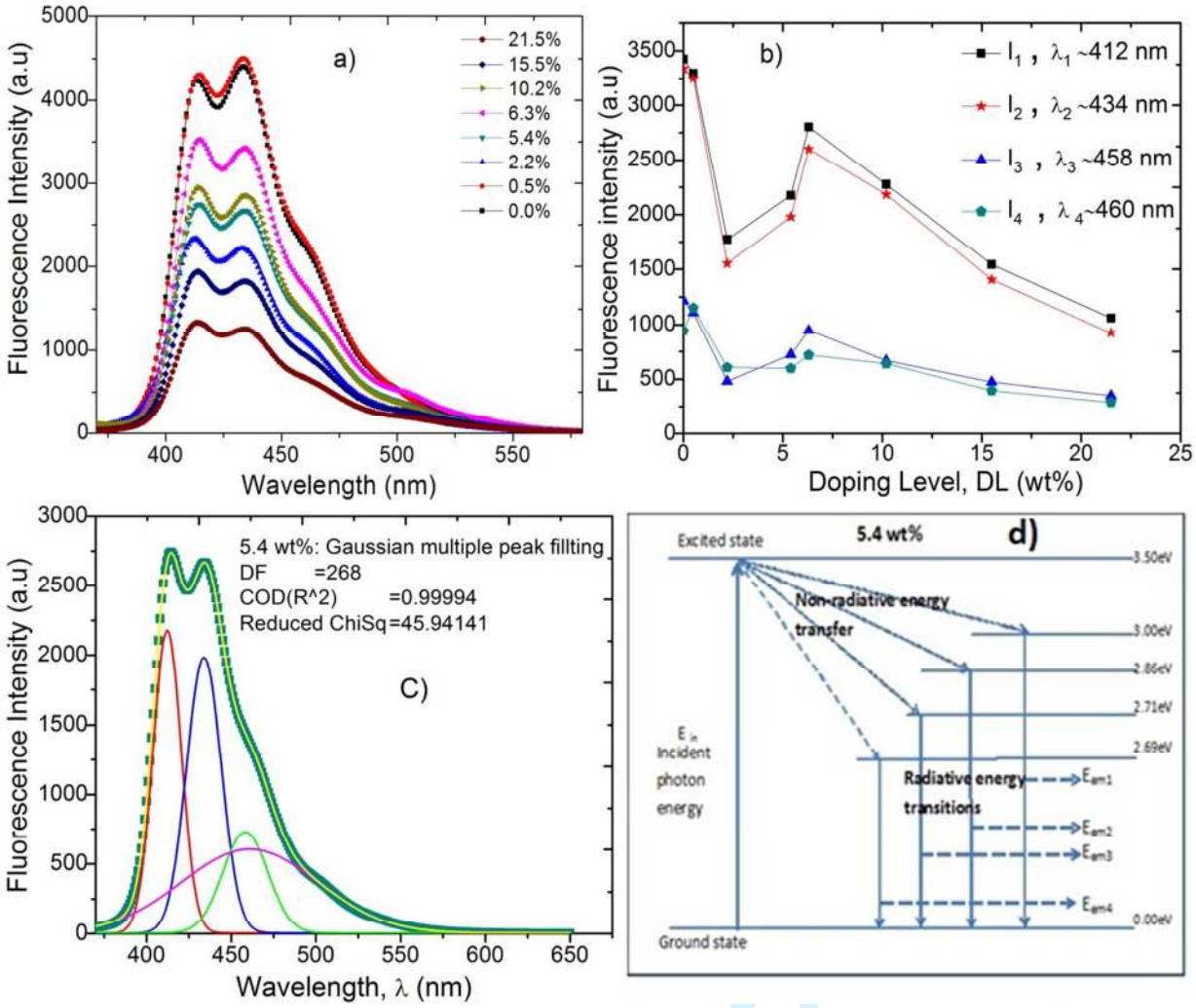

Figure 6: a) Emission spectra at different concentration of $CdCl_2$ in PVA-PVP blend. b) The variation of peak intensity at four different wavelengths. c) Multiple peaks fitting at 5.4 wt% using Gaussian model. d) Simplified Jablonskii diagram at 5.4 wt% doping level of $CdCl_2$ in PVA-PVP blend.

The emission spectra, at various concentrations of $CdCl_2$ in films of PVA-PVP blend (above 0.5 wt% doping level) reveals a quenching effect of the fluorophore (see fig. 6b). This could be due to the transfer of electrons from PVA/ PVP to the cadmium ions (and resulting in formation of Cd atoms). Thus, these electrons of the polymeric host are not available for radiative transition. Another reason for fluorescence quenching could be close proximity of chromophores to the surface of Cd nanostructures. i.e., if the chromophore of PVA-PVP is about 5 nm from the surface of metal (Cd) nanoparticles, excited electrons from chromophores (i.e., non-bonding electrons of oxygen in C=O group) gets tranferred to Cd nanostructures, and hence the fluorescence quenching takes place via non-radiative pathways. Fluorescence enhancement can be achieved by maintaning a distance of 10 nm or more between the chromophore and the surface of Cd nano-structures, because in this situation the Cd nano-structures will have less

interaction with chromophores of the polymer molecules (PVA/ PVP). Hence, a reduction in fluorescence intensity is observed in the latter case.

The energy transfer could take place in two ways; radiative energy transfer, in which the fluorophore deexcites from excited state to ground state by emission of a photon and by non-radiative energy transfer, in which, during the de-excitation process from a metastable state the fluorophore loses its energy by transferring it to its surrounding medium. These radiative and non-radiative energy transitions occur in different energy regions. These are illustrated (for 5.4 wt% doping level) in the simplified Jablonskii diagram (see fig. 6d). PVP has a crucial character, that of encapsulating metal (Cd) nano particles and thus, it acts as capping agent by transferring electron from rigid pyrrolidone group to cadmium ion to form cadmium atom, as explained in reaction scheme shown in fig. 2. Hence, fluorescence quenching is observed in the $CdCl_2$ doped PVA-PVP blend films. The non-radiative energy transfer from PVA-PVP matrix to cadmium atoms results in fluorescence quenching due to the close proximity of chromophores from the surface of Cd nanostructures.

Conclusions

FT-Raman and FTIR spectral analysis of pure and $CdCl_2$ doped PVA-PVP blend films reveals the inter/intra-molecular interactions via hydroxyl (OH) and carbonyl (C=O) group of PVA/ PVAc and PVP with the Cd^+ and Cl^- ions of the dopant. A possible reaction scheme for the interaction of $CdCl_2$ with PVA and PVP molecules has been proposed. From the EDS spectra, evidence for the presence of $CdCl_2$ in polymer matrix is seen, and increased intensity of Cd and Cl x-ray fluorescent peaks is observed with increased content of $CdCl_2$. SEM images give evidence for formation of Cd nanostructures in $CdCl_2$ doped PVA-PVP films. From the UV-Vis spectra, an absorbance hump is seen at 370 nm in $CdCl_2$ doped PVA-PVP blend films, for doping levels between 0.5 wt% and 2.2 wt%, and the possibility of attributing this to LSPR by self-formed Cd metal nanospheres and nanorods has been discussed. The study of fluorescence spectra reveals that there is fluorescence quenching in PVA-PVP blend due to transfer of electrons from polymer molecules to Cd^{2+}, ultimately resulting in formation of Cd nanostructures in the doped film.

Acknowledgements:
The facilities at University Science Instrument Centre (USIC), Karnatak University, Dharwad (KUD) have been used for recording the Raman, FTIR, UV/VIS and fluorescence spectra. We extend our thanks to Sophisticated Test and Instrumentation Centre (STIC), STIC-SAIF, Cochin University, Kochi (Kerala, India) for the SEM images. B. M. Baraker thanks KUD for the UPE fellowship.

References

[1] J.Y. Song, Y.Y. Wang, and C.C. Wan. J. Power Sources **77**, 183 (1999). doi:10.1016/S0378-7753(98)00193-1

[2] A.L. Gopalan, P. Santhosh, K.M. Manesh, J.H. Nho, S. Chul-Gyun Hwang, and K.P. Lee. J. Membr. Sci. **325**, 683 (2008). doi: 10.1016/j.memsci.2008.08.047

[3] B.P. Tripathi and V.K. Shahi. Prog. Polym. Sci. **36,** 945 (2011). doi: 10.1016/j.progpolymsci.2010.12.005

[4] A. Bhide and K. Hariharan. Eur. Polym. J. **43**, 4253 (2007). doi: 10.1016/j.eurpolymj.2007.07.038

[5] N.A. Choudhary, S. Sampath, and A.K. Shukla. Energy Environ. Sci. **2**, 55 (2009). doi: 10.1039/b811217g

[6] Y. Pavani, M. Ravi, S. Bhavani, A.K. Sharma, and V.V.R.N. Rao. Polym. Eng. Sci. **52**, 1685 (2012). doi: 10.1002/pen.23118

[7] L.G. Gilman. Solid solutions of lithium perchlorate in polymer. US Patent. US 3148097 A (1964). https://www.google.com/patents/US3148097

[8] M.R. Ranganath, R.V. Patil, and B. Lobo. Morphological modifications in potassium permanganate doped poly (vinyl alcohol) films. *In* Proceedings of the International Workshop on Applications of Nanotechnology to Energy, Environment and Biotechnology. ISBN: 978-81-920274-0-1, St. Aloysius College (Autonomous), Mangalore, India. December 14- 16, 2010. p 82-88. doi: 10.13140/RG.2.1.2312.1125

[9] H.M. Zidan. J. Appl. Polym. Sci. **88**, 1115 (2003). doi: 10.1002/app.12123

[10] P.K. Khare, S.K. Paliwal, R. Kuraria, H.L. Vishwakarma, A. Verma, and S.K. Jain. Bull. Mater. Sci. **21,** 139 (1998). doi: 10.1007/BF02927562

[11] R.V. Patil, M.R. Ranganath, and B. Lobo. AIP Conf. Proc. **1591**, 183 (2014). doi: 10.1063/1.4872537

[12] D. Vanitha, S.A. Bahadur, N. Nallamuthu, S. Athimoolam, and A. Manikandan. J. Inorg. Organomet. Polym. Mater. **27**, 257 (2017). doi: 10.1007/s10904-016-0468-6

[13] M.R. Ranganath and B. Lobo. Study of the UV- Visible absorption spectra of aqueous ferric chloride doped polyvinylalcohol – polyvinylpyrrolidone blend films. *In* Abstract Book of the International Conference on Condensed Matter Physics. *Edited by* B.K. Sharma, J.V. Yakhmi et al. ISBN: 81-903610-3-1, University of Rajasthan, Jaipur, India. November 25-28, 2007. p 118. doi: 10.13140/RG.2.1.2298.2888

[14] D. Sayala. Composite materials and techniques for neutron and gamma radiation shielding. US Patent. US 7250119 B2 (2007). https://www.google.com/patents/US7250119

[15] R.G. Hoff, N.E. Huston, and C.W Wheelock. Method and apparatus for reactor safety control. US Patent. US 2987455 A (1961). https://www.google.com/patents/US2987455

[16] T.C. Jennings and W.H. Starnes Jr., PVC Stabilizers and Lubricants *In* PVC Handbook, ISBN: 9781569903797, *Edited by* C.E Wilkes, J. W. Summers and C. A. Daniels, Hanser Verlag, p 149, 2005. http://files.hanser.de/hanser/docs/20050818_2581819739-53_3-446-22714-8_Inhalt.pdf

[17] M.I. Sarwar, S. Rafiq, S.M. Yousaf, and Z. Ahmad. Int. J. Polym. Mater. Polym. Biomater. **41**, 185 (1998). doi: 10.1080/00914039808041043

[18] W. Khan and Z. Ahmad. Polym. Degrad. Stab. **53**, 243 (1996). doi: 10.1016/0141-3910(96)00078-x
[19] B.M. Baraker and B. Lobo. Indian J. Pure Appl. Phys. **54**, 634 (2016). http://nopr.niscair.res.in/bitstream/123456789/35893/1/IJPAP%2054(10)%20634-640.pdf
[20] B.M. Baraker and B. Lobo. Microstructure of cadmium chloride doped PVA/PVP blend films. *In* Abstract book of the International Conference on Advanced Materials and Applications, B.M.S. Engineering College, Bengaluru, India. June 15-17, 2016. p 129.
[21] B.M. Baraker, P.B. Hammannavar, and B. Lobo. AIP Conf. Proc. **1665,** 070037 (2015). doi: 10.1063/1.4917901
[22] M.B. Nanda Prakash, A. Manjunath, and R. Somashekar. Adv. Condens. Matter Phys. **2013**, Article ID 690629 (2013). doi: 10.1155/2013/690629
[23] M. Pandey, G.M. Joshi, K. Deshmukh, and J. Ahmad. Adv. Mater. Lett. **6**, 165 (2015). doi: 10.5185/amlett.2015.5639
[24] M. Pandey, G.M. Joshi, and A.R. Polu. Karbala International Journal of Modern Science **1**, 194 (2015). doi: 10.1016/j.kijoms.2015.10.009
[25] M.W. Urban. Fourier Transform Infrared and Fourier Transform Raman Spectroscopy of Polymers (Chapter 1) *In* Structure-Property Relations in Polymers, ISBN: 0-8412-2525-7, *Edited by* M. W. Urban and C. D. Craver, Advances in Chemistry; American Chemical Society (ACS) Publications, Washington, DC, Volume 236, p 3, 1993. doi: 10.1021/ba-1993-0236.ch001
[26] S.P. Mondal, A. Dhar, S.K. Ray, and A.K. Chakraborty. J. Appl. Phys. **105**, 084309 (2009). doi: 10.1063/1.3111971.
[27] E. Rani, R. Aggarwal, A. A. Ingale, K. Bapna, C. Mukherjee, M. K. Singh, P. Tiwari, and A. K. Srivastava. J. Mater. Sci. **51**, 1581 (2016). doi: 10.1007/s10853-015-9481-3.
[28] N. Tanaka, K. Ito and H. Kitano. Macromol. Chem. Phys. **195**, 3369 (1994). doi: 10.1002/macp.1994.021951008
[29] S. Roy. J. Appl. Polym. Sci. **110**, 2693 (2008). doi: 10.1002/app.28332.
[30] V.G Plotnichenko, Yu.A. Mityagin, and L.K. Vodop'yanov. Fiz. Tverd. Tela **19**, 1706 (1977). https://inis.iaea.org/search/search.aspx?orig_q=RN:9412867
[31] J-Y. Zhang, X-Y. Wang, M. Xiao, L. Qu, and X. Peng. Appl. Phys. Lett. **81**, 2076 (2002). doi: 10.1063/1.1507613.
[32] C. Trallero-Giner, A. Debernardi, M. Cardona, E. Menéndez-Proupín, and A. I. Ekimov. Phys. Rev. B **57,** 4664 (1998)**.** doi: 10.1103/PhysRevB.57.4664
[33] Y.A. Badr, K.M. Abd El-Kader, and R.M. Khafagy. J. Appl. Polym. Sci. **92**, 1984(2004). doi: 10.1002/app.20017
[34] B.H. Stuart. Vib. Spectrosc. **10**, 79 (1996). doi: 10.1016/0924-2031(95)00042-9
[35] B. Fanconi. Annu. Rev. Phys. Chem. **31,** 265 (1980). doi: 10.1146/annurev.pc.31.100180.001405.
[36] X. Qi, X. Yao, S. Deng, T. Zhou, and Q. Fu. J. Mater. Chem. A **2,** 2240 (2014). doi: 10.1039/C3TA14340F
[37] S. Krimm, C.Y. Liang, and G.B.B.M. Sutherland. J. Polym. Sci., Part A: Polym. Chem. **22**, 227 (1956). doi: 10.1002/pol.1956.1202210106
[38] M. Ravi, Y. Pavani, K. Kiran Kumar, S. Bhavani, A.K. Sharma, and V.V.R.N. Rao. Mater. Chem. Phys. **130**, 442 (2011). doi: 10.1016/j.matchemphys.2011.07.006
[39] S. Link and M.A. El-Sayed. J. Phys. Chem. B **103**, 8410 (1999). doi: 10.1021/jp9917648
[40] P. Mulvaney. Langmuir **12**, 788 (1996). doi: 10.1021/la9502711

[41] N. Nath and A. Chilkoti. Anal. Chem. **76**, 5370 (2004). doi: 10.1021/ac049741z
[42] J. Zheng, C. Zhang, and R. M. Dickson. Phys. Rev. Lett. **93**, 077402 (2004). doi: 10.1103/PhysRevLett.93.077402
[43] W. Fritzsche and T.A. Taton. Nanotechnology **14**, R63 (2003). doi: 10.1088/0957-4484/14/12/R01
[44] S.O. Obare, R.E. Hollowell, and C.J. Murphy. Langmuir **18**, 10407 (2002). doi: 10.1021/la0260335
[45] N. Nath and A. Chilkoti. Proc. SPIE **4626,** 441 (2002). doi: 10.1117/12.472110
[46] J-M. Nam, C.S. Thaxton, and C.A. Mirkin. Science **301**, 1884 (2003). doi: 10.1126/science.1088755
[47] C.J. Murphy and N.R. Jana. Adv. Mater. (Weinheim, Ger.) **14**, 80 (2002). https://www.researchgate.net/publication/228556843
[48] E. Hutter and J.H. Fendler. Adv. Mater. (Weinheim, Ger.) **16**, 1685 (2004). doi: 10.1002/adma.200400271
[49] B.S. Amma, K. Manzoor, K. Ramakrishna, and M. Pattabi. Mater. Chem. Phys. **112**, 789 (2008). doi: 10.1016/j.matchemphys.2008.06.043
[50] D. Patra and A.K. Mishra. Sens. Actuators, B **80**, 278 (2001). doi: 10.1016/S0925-4005(01)00919-4

Table 1: FT-Raman and FTIR peak assignments, for pure and $CdCl_2$ doped PVA-PVP films.

Peak Assignment	Raman Assignments Wavenumber (cm^{-1})		FTIR Assignments Wavenumber (cm^{-1})	
	Pure PVA-PVP	Doped PVA- PVA	Pure PVA-PVP	Doped PVA- PVA
O-H stretching	…	…	3440	3424-3448
Asy CH_2 stretch, chain	…	2987	2960	2966-2969
Sy CH_2 stretch, chain	2921	2921-2925	2924	2922-2926
C-H stretch	….	2832-2857	2856	2848-2856
C=O stretching (acetyl group/ PVAc)	1732	1710-1735	1734	1732-1744
C=O stretching(s); PVP	1652	1632-1665	1651	1627-1636
C-N stretch	1528	1513-1594	1500	1500-1562
C-O stretch or CH_2 scissor	1436	1436-1444	1460	1413-1467
C-H bend	1360	1360-1375	1380	1356-1391
CH-OH bending	1301	1301-1317	….	….
C-N , C-H_2 wagging	1229	1201-1260	1262	1260-1271
as C-OH valence ring vibrations, C-O-C stretch	1116	1113-1180	1103	1095-1124
C-N vibrations	….	---	1030	1021-1043
C-C , ring breathing	927	923-939	930	…..
C-C Ring	849	848-854	850	801-861
C-C chain, C=O bending	750	747-762	740	702-718
N-C=O bend, ring def	551, 630	515, 640	550, 650	515, 613
Out of plane vibration	451	430-490	421	425-430
Di-substituted acetylene	355	355-390	…	…
CH_3 twisting, C-C-C def	220	220-265	…	…
υ_{LO}	179	178-183	…	…

Table 2: Intensity (I_i), wavelength (λ_i) and full width half maximum (FWHM) for four different (i= 1 to 4) emission (fluorescence) peaks, from multiple Gaussian fitting at a different dopant concentration of $CdCl_2$ in PVA-PVP blend. The excitation wavelength is 355 nm.

$CdCl_2$ (wt%)	0.0	0.5	2.2	5.4	6.3	10.2	15.5	21.5
λ_1 (nm)	411.6±0.05	412.0±0.06	411.0±0.06	412.3±0.053	412.3±0.061	412.1±0.039	411.8±0.04	412.0±0.053
I_1 (a.u)	3425.3±0.01	3296.8	1774.1	2174.8	2803.8	2275.7	1541.7	1061.1
$FWHM_1$ (nm)	17.0±0.07	16.9±0.08	17.0±0.07	16.7±0.06	16.6±0.07	15.9±0.05	16.8±0.01	17.1±0.06
λ_2 (nm)	433.5±0.05	433.6±0.06	433.4±0.07	434.0±0.07	434.0±0.07	434.4±0.05	434.2±.06	434.0±0.06
I_2 (a.u)	3328.7	3248.6	1552.1	1979.9	2602.2	2184.4	1406.1	923.2
$FWHM_2$ (nm)	19.8±0.18	19.8±0.21	20.4±0.23	20.5±0.21	20.6±0.24	21.4±0.18	21.3±0.02	20.6±0.22
λ_3 (nm)	457.7±0.32	458.4±0.35	458.7±0.38	458.3±0.39	458.2±0.44	460.7±0.29	459.5±0.32	458.4±0.37
I_3 (a.u)	1217.2	1108.7	481.3	725.2	945.9	668.4	474.2	348.4
$FWHM_3$ (nm)	25.4±0.46	24.7±0.53	23.4±0.54	26.5±0.51	26.2±0.54	23.9±0.40	24.5±0.45	26.4±0.45
λ_4 (nm)	459.3±0.26	454.1±0.21	448.5±0.16	461.0±0.22	464.5±0.27	456.2±0.17	463.3±0.22	462.8±0.19
I_4 (a.u)	942.8	1150.6	606.9	599.1	720.38	641.9	396.9	287.9
$FWHM_4$ (nm)	73.5±0.43	71.7±0.44	79.6±0.49	81.2±0.41	84.0±0.45	80.7±0.4	87.4±0.35	90.3±0.39